MAGNETIC FIELDS IN STAR-FORMING MOLECULAR CLOUDS: JCMT POLARIMETRY OF OMC-3 IN ORION A

B. C. Matthews and C. D. Wilson

Department of Physics & Astronomy, McMaster University, 1280 Main St. W., Hamilton, ON L8S 4M1, Canada

Abstract

The first polarization map of the OMC-3 region in Orion A's Integral Filament is presented. Using the new imaging polarimeter mounted on SCUBA at the James Clerk Maxwell Telescope, we have detected thermal emission at 850 μm from dust along the 6$'$ length of the dense filament. The polarization pattern is highly ordered and is aligned with the long axis of the filament throughout most of the region, diverging only near the southern boundary by $30 - 50°$. This configuration indicates a plane-of-sky magnetic field, $B_\perp$, oriented normal to the filament along most of its length whether the polarization arises from thermal emission of dust grains aligned by the magnetic field via paramagnetic inclusions or radiative torques. The mean percentage polarization measured is 4.2% with a 1σ dispersion of 1%. Depolarization effects, as previously detected in many other star-forming cores and protostars, are also detected toward the densest parts of the filament.

Key words: ISM: clouds, magnetic fields, molecules – polarization – Stars: formation – submillimeter – OMC-3

1. Introduction

The role of magnetic fields in the evolution of molecular clouds and their associated star formation has been well-established in recent years (e.g. Heiles et al. 1993). Fields provide support for clouds against gravity on large and small scales and could provide the means for shaping cloud cores (Fiege & Pudritz 2000). At a distance of 500 pc, the Orion complex is the closest star-forming region currently undergoing massive star formation, and as such, has been the object of intense study. The massive dense core, OMC-1, which lies behind the Orion Nebula, has been the most deeply studied. This core is embedded in the integral-shaped filament, identified in ^{13}CO $J = 1-0$ by Bally et al. (1987) and most recently mapped at 850 and 450 μm by Johnstone & Bally (1999). The OMC-3 region lies at the northern tip of the filament (Bally et al. 1987), near the HII region NGC 1977 (see Kutner et al. 1976). Molecular studies reveal the dust temperatures to be considerably cooler (T $\sim$ 20-25 K) in the OMC-3 region than in OMC-1 (Chini et al. 1997).

Dust condensations in OMC-3 were identified in 1.3 mm continuum by Chini et al. (1997). An evolutionary sequence has been suggested, with source ages declining to the north of OMC-1. Reipurth et al. (1999) have done a VLA search at 6 cm for compact sources in the region and report no sources coincident with the positions of MMS1 and MMS4, two of the most northern condensations identified by Chini et al. (1997). Additionally, there is no outflow associated with either source (Yu et al. 1997; Chini et al. 1997; Caslets & Langer 1995). These results suggest that these objects may in fact be in a pre-collapse phase, since outflows are known to be associated with the earliest phases of collapse (Shu et al. 1987).

Goodman et al. (1995) illustrated that measurements of polarization of background starlight in the optical and near-infrared are not effective tracers of magnetic field structure in dense molecular gas due to poor alignment and/or amorphous dust grain structure. At submillimeter and millimeter wavelengths, aligned, rotating grains produce polarized thermal emission. Draine & Weingartner (1996, 1997) have shown that radiative torques are highly effective at aligning grains of specific sizes ($\sim$0.2 μm). Lazarian et al. (1997) suggest that the effects of radiative torques could be comparable to paramagnetic inclusions (Purcell 1975, 1979; Spitzer et al. 1979) at aligning grains in the star-forming interstellar medium. Both these mechanisms result in grains aligned with their long axes perpendicular to the magnetic field.

Here, we present polarimetry data of OMC-3. These data represent the first polarimetry of this active star-forming region and are also some of the first obtained with the new imaging polarimeter at the James Clerk Maxwell Telescope (JCMT).

2. 850 micron polarization

Figure 1 shows the polarization pattern along OMC-3. The greyscale indicates the uncalibrated total intensity. The vectors are highly ordered and follow the filament's orientation along most of its length. Thus, the orientation of the $B_\perp$ field is predominantly orthogonal to the filament. The regions of highest S/N are indicated by contours. The JCMT polarimeter and data reduction method are discussed in Matthews & Wilson (2000).

On each histogram, the dashed line represents the position angle of the *filament* while the polarization data have

Proc. of 33rd ESLAB Symp. *"Star formation from the small to the large scale"* (F. Favata, A. A. Kaas & A. Wilson eds., ESA SP-445, 2000)

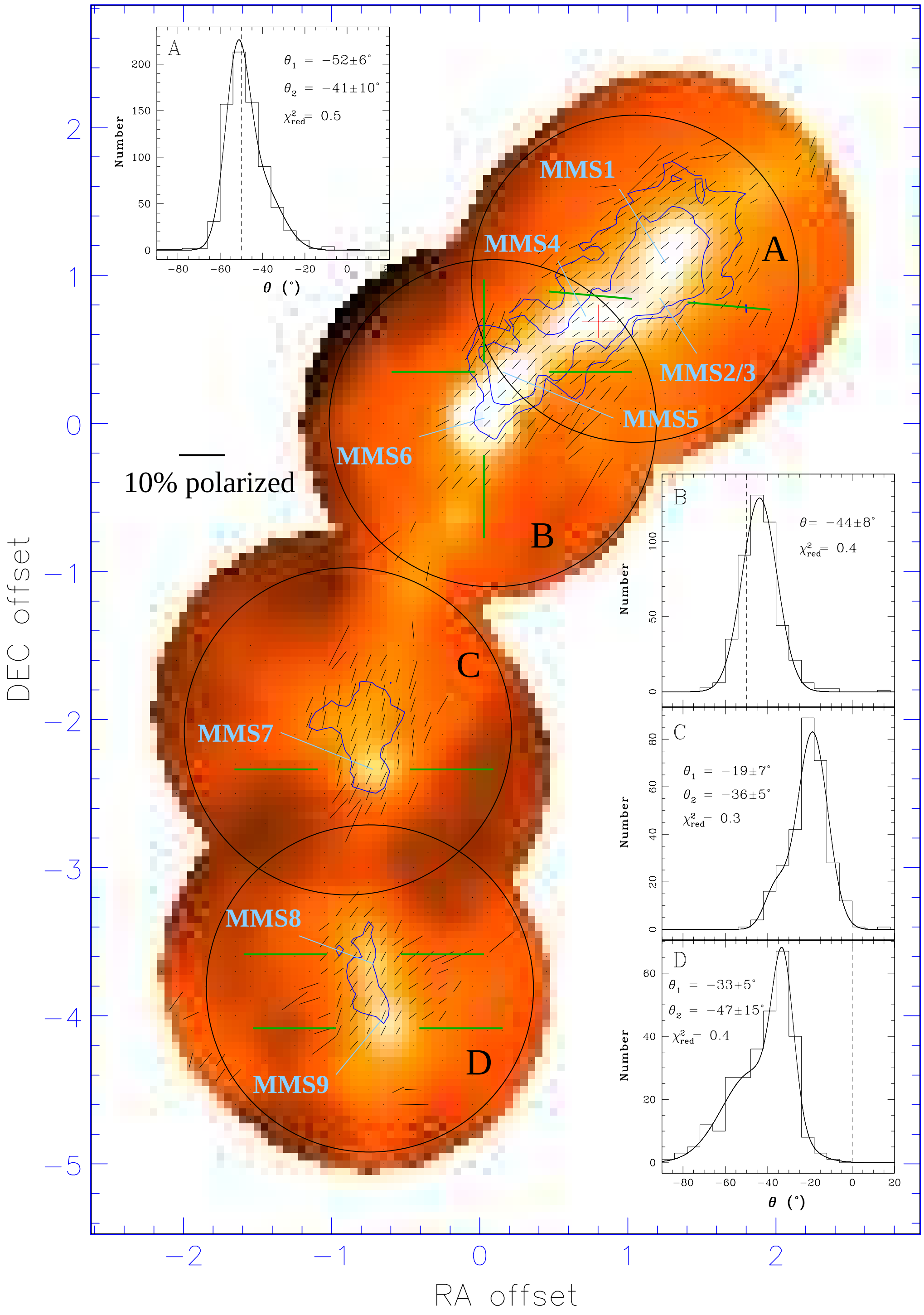

Figure 1. 850 μm polarization structure along OMC-3. The coordinates are arcminute offsets from the position of MMS6, $\alpha_{1950} = 5^h32^m55.6^s$ and $\delta_{1950} = -5°03'25''$. Greyscale indicates variations in uncalibrated I, with a range of -2 to 3 σ. Polarization vectors are overlain where $p < 20\%$ and σ_p, the signal-to-noise of polarized flux, > 2.5. Contours indicate bounds of $\sigma_p = 6$ ($d\theta < 5°$) and $\sigma_p = 10$ ($d\theta < 3°$) respectively. These data contain $6\sigma_p$ detections on sources as weak as 0.5 Jy. MMS1–9 mark the positions of dust condensations. The orientations of known outflows have been indicated by straight lines on either side of the outflow source. The cross shows the centre of the cut shown in Figure 3. Subregions, labelled A through D, are identified, and the distributions of position angle for each are shown in the corresponding histograms.

been binned to 6° widths and fit with 1 or 2 Gaussians as appropriate by minimizing chi-squared. Only values with $\sigma_\theta < 12°$ are plotted. We report the mean and 1 σ dispersion of each Gaussian. The data reveal the changing orientation of the polarization pattern with respect to the filament. In regions A through C, the vectors are roughly aligned with the filament to within $\pm 10°$; but in region D, the filament is aligned north-south, with polarization vectors offset by $30 - 50°$. Figure 1 shows the outflow directions inferred from CO and H_2 shocks. The source designated MMS9 has been identified as possessing the most powerful outflow in the region (Reipurth et al. 1999); and if it is indeed older than the more northern sources as suggested by Chini et al. (1997), then its outflow could have had enough time to influence the magnetic field direction in its vicinity. However, the outflow direction is offset from $B_\perp$ by $30 - 50°$, so this relationship remains unclear.

3. Percentage Polarization

Unfortunately, p does not reveal the magnitude of $B_\perp$, since it is dependent on grain composition, shape and degree of alignment as well as field strength. The median value of 4.2% is comparable to the 4.1% measured at 350 μm in OMC-1 (Schleuning 1998). These two frequencies are both thought to trace thermal emission from dust.

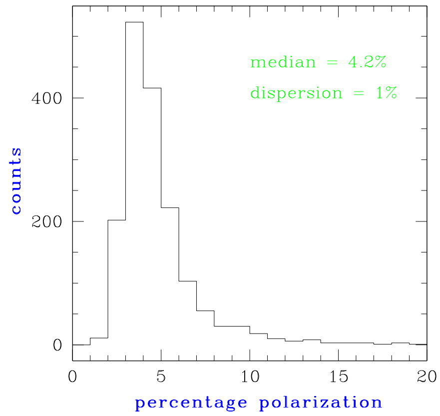

Figure 2. Percentage Polarization. This histogram shows the distribution of percentage polarization, p, along the filament. Only values with $\sigma_p > 2.5$ are plotted; values up to 100% were allowed, but only 27 vectors have $p > 20\%$. Values as high as 11.9% were measured with $\sigma_p > 7$.

4. Depolarization in OMC-3

Observations of "depolarization", or the decrease in percentage polarization toward higher densities, have been made for many protostars. Figure 3 shows a cut perpendicular to the filament at the position of MMS4, indicated by a cross in Figure 1. These measurements of decreased p toward regions of high density could be due to changes in physical conditions or averaging of small scale variations in a large beam, but they are also suggested as an observable signature of helical fields (Fiege & Pudritz 2000). In OMC-1, Schleuning (1998) has measured a decreased polarization toward the core centre at 350 μm and high-resolution data of the region by Rao et al. (1998) with BIMA revealed substantial changes in polarization angle near the source which would tend to average to zero in a larger beam. The interpretation of this depolarization effect in OMC-3 will require modelling of field structures.

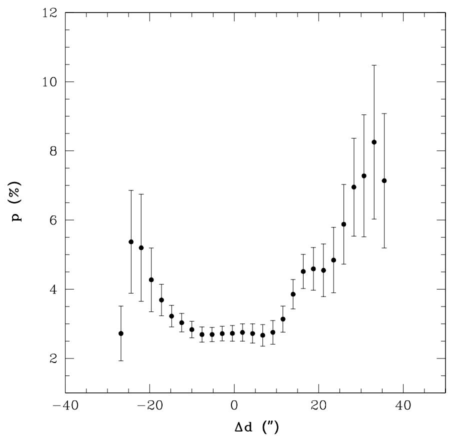

Figure 3. Depolarization across MMS4. These data are centred on $\alpha_{1950} = 5^h32^m52.5^s$ and $\delta_{1950} = -5°02'46''$, the position of the cross in Figure 1. Δd is the offset perpendicular to the filament. The plot clearly shows a reduction in polarization toward the centre of the filament. The error bars represent the uncertainty associated with each interpolated data point.

5. Summary and Future Work

We have obtained the first polarimetry of the OMC-3 region in Orion A. The polarization pattern aligns well with the filament, diverging only near the southern tip. Outflow directions do not align consistently with either the filament nor the $B_\perp$ direction, indicating that the field of the filament is thus unlikely to be the dominant factor in determining the configuration of the protostellar systems embedded within it. A mean percentage polarization of $4.2 \pm 1\%$ is detected, with a significant depolarization effect across the filament at the position of MMS4.

In addition to these data, we have observed clouds in Orion B, ρ Ophiuchus and Perseus' B1 cloud. In future publications, we will be able to compare polarization structures across different regions. In addition, the availability of new models for filamentary molecular clouds will allow us to test how well the predicted polarization pattens agree with those observed. This could provide constraints on field strengths or grain models (where field strength can be independently established).

References

Bally, J., Langer, W.D., Stark, A.A., 1987, ApJ, 313, L45

Caslets, A., Langer, W.D., 1995, A&A, 294, 835

Chini, R., Reipurth, B., Ward-Thompson, D., et al. 1997, ApJ, 474, L135

Draine, B.T., Weingartner, J.C., 1996, ApJ, 470, 551

Draine, B.T., Weingartner, J.C., 1997, ApJ, 480, 633

Fiege, J., Pudritz, R., 2000, MNRAS, 311, 85

Goodman, A.A., Jones, T.J., Lada, E.A., Myers, P.C., 1995, ApJ, 448, 748

Heiles, C., Goodman, A.A., McKee, C.F., Zweibel, E.C., 1993, in *Protostars & Planets III*, ed. E.H. Levy and J.I. Lunine (Tucson, University of Arizona Press), 279

Johnstone, D., Bally, J., 1999, ApJ, 510, L49

Kutner, M.L., Evans, N.J., Tucker, K.D., 1976, ApJ, 209, 452

Lazarian, A., Goodman, A.A., Myers, P.C., 1997, ApJ, 490, 273

Matthews, B.C., Wilson, C.D., 2000, ApJ, in press

Purcell, E.M. 1975 in *Dusty Universe*, ed. G.B. Field & A.G.W. Cameron (New York: Neal Watson), 155

Purcell, E.M. 1979, ApJ, 231, 404

Rao, R., etc., 1998, 502, L75

Reipurth, B., Rodríguez, L.F., Chini, R., 1999, AJ, 118, 983

Schleuning, D.A., 1998, ApJ, 493, 811

Shu, F.H., Adams, F.C., Lizano, S., 1987, ARAA, 25, 23

Spitzer, L., Jr., McGlynn, T.A., 1979, ApJ, 231, 417

Yu, K.C., Bally, J., Devine, D., 1997, ApJ, 485, L45